

We are IntechOpen, the world's leading publisher of Open Access books Built by scientists, for scientists

6,900

Open access books available

185,000

International authors and editors

200M

Downloads

Our authors are among the

154

Countries delivered to

TOP 1%

most cited scientists

12.2%

Contributors from top 500 universities



WEB OF SCIENCE™

Selection of our books indexed in the Book Citation Index
in Web of Science™ Core Collection (BKCI)

Interested in publishing with us?
Contact book.department@intechopen.com

Numbers displayed above are based on latest data collected.
For more information visit www.intechopen.com



Rotor Speed Stability Analysis of a Constant Speed Wind Turbine Generator

Mitalkumar Kanabar and Prof. Srikrishna Khaparde
Indian Institute of Technology Bombay
India

1. Introduction

As wind turbine generator (WTG) technology is one of the fastest growing renewable energy technologies, the focus is given towards the cost-benefit analysis (Agalgaonkar et al., 2006); as well as, study of its specific grid integration issues (Zavadil et al., 2005). Many countries have their own grid codes (rules and regulations) to integrate WTG into the utility grid. Most common grid codes for WTG include low voltage ride through (LVRT) capability, voltage control, power quality, and protection requirements. AWEA recommended adoption of an LVRT requirement developed by E.ON Netz as shown in Fig. 1. Whereas, WECC (Western Electricity Coordinating Council) has put effort to lenient this stringent requirement in May 2005.

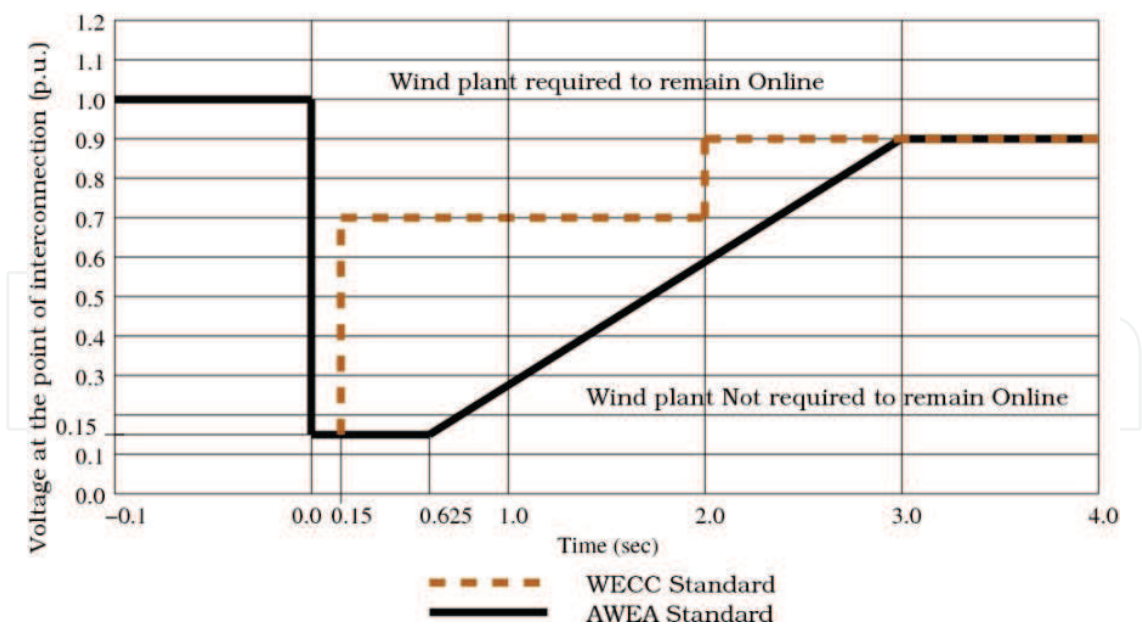


Fig. 1. LVRT requirements for wind generation facilities [4].

There are two major types of WTG technology: constant speed WTG and variable speed WTG (Ackermann, 2005). The major earlier installations in developing countries are based on the constant speed WTG technology because it is robust, economical, and simple in design (Kanabar & Khaparde, 2008). India ranks fifth in the world with a total installed

capacity of more than 11,500 MW by the end of March, 2010 (Wind Power, 2010). Most of the WTGs currently installed in India are fixed or constant speed induction generators. However, unlike variable speed WTG, the constant speed WTG does not satisfy LVRT requirements that are because during a nearby fault, rotor accelerates to very high value and hence the WTG becomes unstable (Kanabar et al., 2006). This phenomenon is referred to as rotor speed instability (Samuelsson & Lindahl, 2005).

Several literatures are available on stability analysis of a constant speed WTG. The study of transient stability of a constant speed WTG using dynamic simulation has been presented in (Rodriguez et al., 2002) with case study on Spanish system. The comparison of transient stability margin between constant speed and variable speed WTGs has been discussed in (Nunes et al., 2003). It has been shown that a constant speed WTG has a much lesser transient stability margin as compared with a variable speed WTG. Reference (Chompoo-inwai et al., 2005) examines the response of a constant speed WTG during faults and the possible impacts on the system stability when the percentage of wind generation increases. Moreover, literature also suggests controlling wind turbine blade angles to stabilize the generator during fault conditions. A comparative study between active stall control and pitch control of a constant speed WTGs are discussed in (Ackermann, 2005). It can be concluded from the literature that to meet the LVRT requirements (according to grid codes), rotor speed stability margin of a constant speed WTG should be improved. There are two different methods to control a constant speed WTG: 1) providing additional reactive power support for improving the terminal voltage, this in turn, will increase the electromagnetic torque and hence, the rotor acceleration can be reduced; 2) mechanical torque control by pitching the blades during a system disturbance can be used to reduce the rotor acceleration. There are several already installed constant speed WTGs without this blade pitch control functionality. Therefore, first method of providing additional reactive power would be suitable for them. On the other hand, many modern wind turbine blades have pitch control mechanism. And hence, second method would be suitable for them.

Section-2 of the chapter presents the detailed analytical formulae derived for rotor speed stability margin to determine the exact amount of additional reactive power support required to achieve the LVRT capabilities. Using simulation of the dynamic model in MATLAB, it has been shown that the calculated value of reactive power is sufficient for the WTG to comply with the LVRT requirements by enhancing rotor speed stability. Section-3 demonstrates the implementation of the active stall controller for the constant speed WTG enhances, and explains how this method can enhance rotor speed stability to meet the LVRT requirements with the help of simulation using DlgSILENT software.

2. Enhancement of rotor speed stability margin of a constant speed WTG using additional reactive power compensation

A constant speed WTG consumes reactive power and hence, shunt capacitor banks are connected to it to supply reactive power locally. Conventionally, the nominal rating of a capacitor bank selected is to compensate for no-load reactive power demand (Jenkind et al., 2000). However, as real power is exported, additional reactive power is drawn from the network. This reactive power consumption ramps up drastically during faults due to acceleration of the rotor. Consequently, it has to be disconnected from the grid due to rotor speed instability. Therefore, a constant speed WTG without pitch control does not possess LVRT capability. During a fault, if additional shunt capacitor banks are connected, then the

recovery of voltage and electromagnetic torque can be improved. Thereby, rotor acceleration can be reduced. This will increase the critical clearing time of a constant speed WTG. This section will quantify the amount of additional reactive power support required to improve the critical clearing slip and time such that it can meet the LVRT requirements. Further, the effect of wind velocity and rotor inertia constant on the critical clearing slip and time have also been discussed.

2.1 Steady state analysis of a constant speed WTG

Fig. 2 shows a single line diagram of a sample system with a constant speed WTG and capacitor banks connected to an infinite bus through a step-up power transformer.

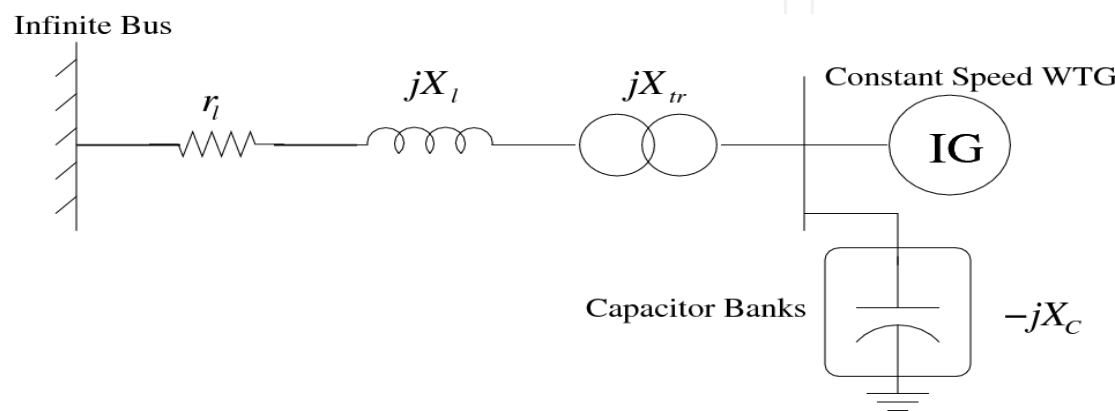


Fig. 2. Single line diagram of a sample system.

To calculate the exact amount of reactive power support required to satisfy the LVRT requirement, it is necessary to obtain a relation between the critical slip (scr) and the reactive power support in steady state.

Let us consider the steady-state equivalent model of a constant speed induction generator as shown in Fig. 3. In this figure, r_l and X_l are the line resistance and reactance respectively; X_{tr} is the transformer reactance; X_C is the capacitive reactance; r_s and X_s are the stator resistance and reactance respectively; X_m is the magnetizing reactance; r'_r and X'_r are the rotor resistance and reactance referred to the stator side respectively and s is the rotor slip. All these above quantities are in per unit.

To obtain the torque-slip characteristics of a constant speed WTG, a Thevenin equivalent has been derived across points A and B, as shown in Figs. 3 and 4.

The formula to calculate the Thevenin's voltage is indicated below:

$$V_{th} = \frac{V X_C X_m}{(r_l + jX_{lt})[r_s + j(X_s + X_m - X_C)] + X_C(X_s + X_m) - jX_C r_s} \tag{1}$$

Where,

$$X_{lt} = X_l + X_{tr}$$

The values of the Thevenin resistance (rth) and Thevenin reactance (xth) are obtained as follows:

$$r_{th} = \frac{a \cdot c + b \cdot d}{c^2 + d^2} \tag{2}$$

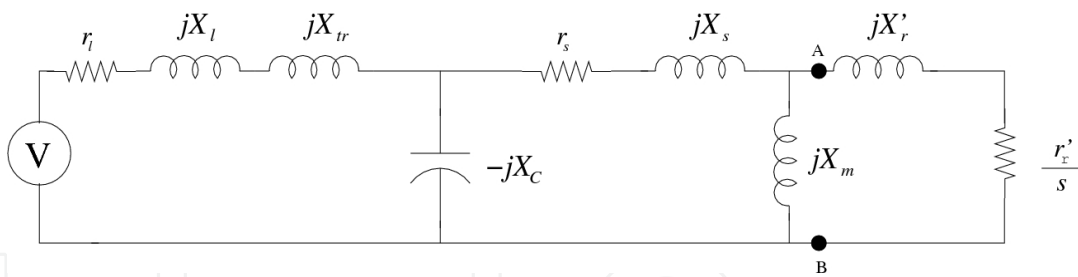


Fig. 3. Equivalent circuit diagram of a sample system.

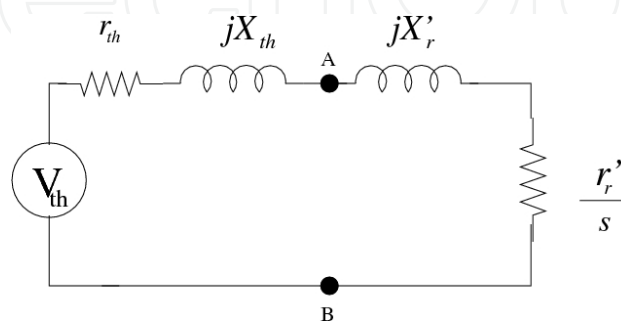


Fig. 4. Thevenin's equivalent circuit.

$$X_{th} = \frac{b \cdot c - a \cdot d}{c^2 + d^2} \quad (3)$$

Where,

$$B_C = \frac{1}{X_C} = \text{Total susceptance of the capacitor banks}$$

$$a = B_C[X_s X_{lt} X_m - r_s r_l X_m] - X_m(X_s + X_{lt})$$

$$b = -B_C[r_l X_s X_m + r_s X_{lt} X_m] + X_m(r_s + r_l)$$

$$c = -B_C[r_l(X_s + X_m) + r_s X_{lt}] + r_s + r_l$$

$$d = B_C[r_s r_l - X_{lt}(X_s + X_m)] + X_s + X_m + X_{lt}$$

From Fig. 4, the electromagnetic torque (in p.u.) of a constant speed WTG can be determined as follows:

$$T_e = \frac{|V_{th}|^2 \cdot \frac{r_r'}{s}}{\left[\frac{r_r'}{s} + r_{th}\right]^2 + [X_r' + X_{th}]^2} \quad (4)$$

Using (6.4), the torque versus slip characteristic has been obtained, and is shown in Fig. 4.4. In the normal operating condition, the electrical and mechanical torques will be equal; hence, the WTG will operate at slip s_0 (point Q). When a severe fault occurs close to the WTG, the terminal voltage of the WTG falls drastically. This will reduce the electrical torque to almost zero. Consequently, the rotor will oscillate, and the slip of the WTG will increase

gradually. Once the fault is cleared, the terminal voltage and electrical torque will again increase to its nominal value and thereby, the rotor will decelerate. If the fault is cleared after the critical clearing time (t_{cr}), the rotor may accelerate to a higher than critical slip (s_{cr}) value. In this case, although the fault is cleared and the terminal voltage is recovered back, the rotor will continue to accelerate (beyond s_{cr}), and therefore, the WTG will enter into the unstable region. This phenomenon implies that if the rotor slips crosses the point P (as shown in Fig 5), the WTG will be disconnected from the grid due to over-speed protection. In practice, over-speed protection circuit disconnects the WTG from the grid when the speed of the WTG exceeds 1.2 p.u.

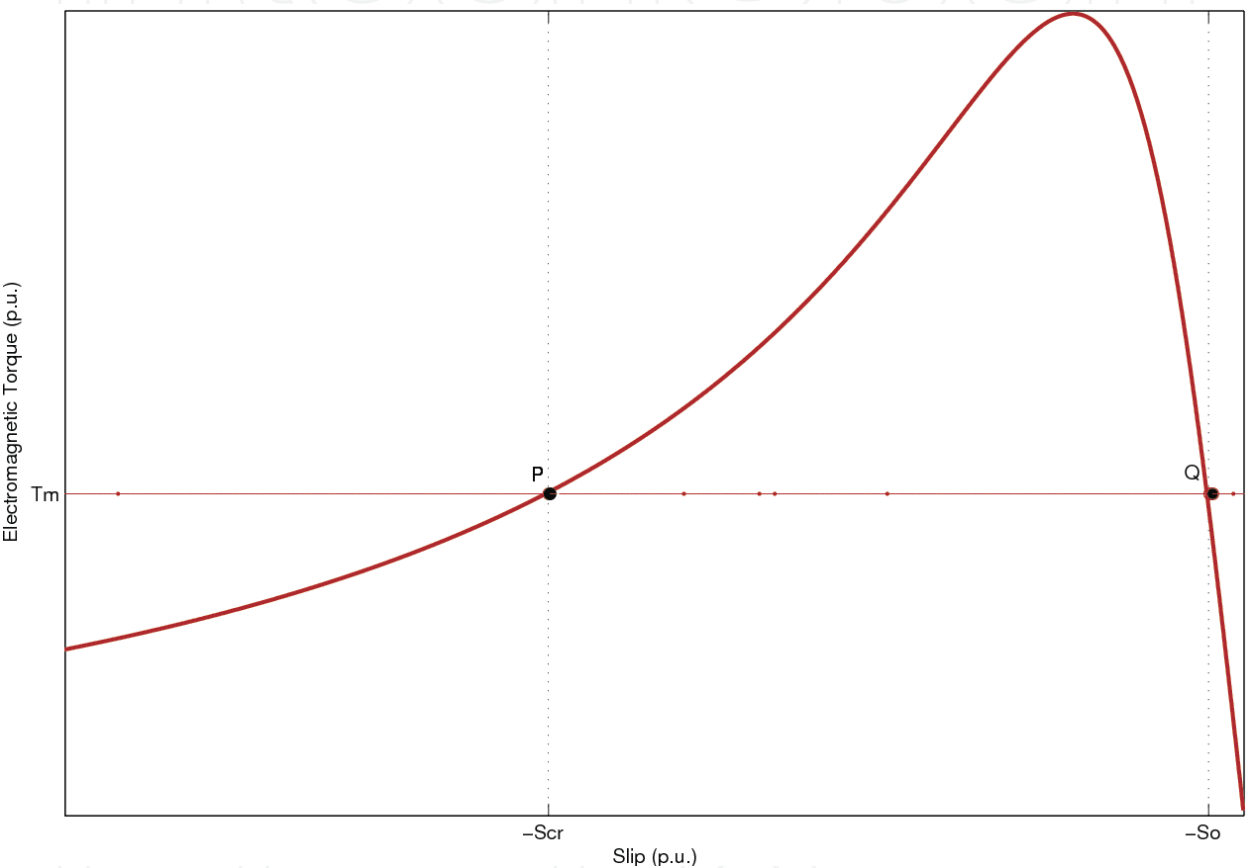


Fig. 5. Torque-slip characteristic of a constant speed WTG.

2.1.1 Evaluation of critical slip

As shown in Fig. 5, the critical slip can be obtained by equating the electrical torque of the WTG with its mechanical torque.
From (4),

$$T_e = \frac{|V_{th}|^2 \cdot \frac{r_r'}{s}}{[\frac{r_r'}{s} + r_{th}]^2 + [X_r' + X_{th}]^2} = T_m \tag{5}$$

This leads to,

$$\frac{|V_{th}|^2}{T_m} \cdot \frac{r_r'}{s} = \left(\frac{r_r'}{s}\right)^2 + 2r_{th} \frac{r_r'}{s} + r_{th}^2 + (X_r' + X_{th})^2 \quad (6)$$

$$\Rightarrow [r_{th}^2 + (X_r' + X_{th})^2] \cdot s^2 + [2r_{th}r_r' - r_r' \frac{|V_{th}|^2}{T_m}] \cdot s + (r_r')^2 = 0$$

This is a quadratic equation in 's', and following are its roots (scr,s0) (as depicted in Fig. 5)

$$s_{cr} = \frac{-[2r_{th}r_r' - r_r' \frac{|V_{th}|^2}{T_m}] + \sqrt{[2r_{th}r_r' - r_r' \frac{|V_{th}|^2}{T_m}]^2 - 4(r_r')^2[r_{th}^2 + (X_r' + X_{th})^2]}}{2[r_{th}^2 + (X_r' + X_{th})^2]} \quad (7)$$

$$s_0 = \frac{-[2r_{th}r_r' - r_r' \frac{|V_{th}|^2}{T_m}] - \sqrt{[2r_{th}r_r' - r_r' \frac{|V_{th}|^2}{T_m}]^2 - 4(r_r')^2[r_{th}^2 + (X_r' + X_{th})^2]}}{2[r_{th}^2 + (X_r' + X_{th})^2]} \quad (8)$$

Equation (7) shows that s_{cr} is mainly a function of the parameters such as r_{th} , X_{th} and V_{th} . The value of these parameters also depends on B_c (the amount of reactive power compensation in per unit).

2.2 Calculation of critical clearing time

Let us consider rotor dynamics to obtain the critical clearing time,

$$\frac{ds}{dt} = \frac{T_m - T_e}{2H} \quad (9)$$

where, s is the slip in p.u., T_m is the mechanical torque in p.u., T_e is the electromagnetic torque in p.u., H is the combined inertia constant of the WTG system in sec. Integration of (9) leads to,

$$\int_0^{t_{cr}} dt = \frac{2H}{T_m - T_e} \int_{s_0}^{s_{cr}} ds \quad (10)$$

It has been assumed that during fault $T_m - T_e$ remains constant. Finally,

$$t_{cr} = \frac{2H}{T_m - T_e} (s_{cr} - s_0) \quad (11)$$

From the above equation, it can be observed that the critical clearing time is directly proportional to the inertia constant and the difference of the critical and initial slip, and inversely proportional to the difference between the mechanical and electromagnetic torque.

2.3 Simulation results and discussions

Modelling of the constant speed WTG, capacitor banks and grid has been carried out in MATLAB/SIMULINK software tool. Currents from the WTG have been added to the currents from the capacitor banks. The total current has been injected into the grid. From

this injected current, the terminal voltage has been calculated which is given as an input to the WTG and capacitor banks.

A 600 kW constant speed WTG has been considered for this analysis. The machine parameters are listed in Table 1. This WTG is stall controlled and hence, it does not possess blade-pitch control.

Parameters	Value
Rated Power	600 kW
Rated Phase Voltage	690 V
Rated Frequency	50 Hz
Number of Poles	4
Stator Resistance (r_s)	0.016 p.u.
Stator Leakage Reactance (X_{ls})	0.15 p.u.
Rotor Resistance (r_r)	0.01 p.u.
Rotor Leakage Reactance (X_{lr})	0.11 p.u.
Magnetizing Reactance (X_m)	7.28 p.u.
Inertia constant (J)	18.029 kg m ²

Table 1. Parameters of a Constant Speed WTG

2.4.1 Effect of additional reactive power support

With the help of simulation, it has been shown that this 600 kW constant speed WTG does not comply with the LVRT requirements (as shown in Fig. 8). Hence, the WTG has to be disconnected from the grid due to rotor speed instability whenever a fault occurs in its vicinity. However, by providing additional reactive power support, rotor speed stability of the WTG can be enhanced such that it can satisfy the LVRT requirements. This phenomenon has been discussed in this section with the help of simulation results. Further, the exact quantification of reactive support required achieving particular values of critical slip and critical clearing time has been obtained theoretically. Finally, using the dynamic model of the system, it has been shown that dynamic simulation results (critical slip and time) match with the analytically calculated results using equations (7) and (11). Fig. 6 shows the torque-slip characteristics of a 600 kW WTG with two different value of reactive power injection. Equation (3) shows that the electromagnetic torque is a function of V_{th} , r_{th} and X_{th} . For a given set of machine parameters, V_{th} , r_{th} and X_{th} are functions of B_C (the value of reactive power compensation) as shown in equations (1), (2) and (3) respectively. For nominal reactive power support, the value of B_C is 0.23 p.u., and with an additional capacitor bank of 0.22 p.u., the value of B_C will be 0.45 p.u. As indicated in Fig. 6, an additional value of B_C will shift the torque-slip characteristic upwards. Consequently, the value of critical slip will increase from -0.118 p.u. to -0.15 p.u. Improvement of s_{cr} because of additional B_C can also be obtained numerically using (7). Similarly, using (11), t_{cr} has been calculated as 0.12 s with the nominal capacitor bank, and 0.155 s with an additional capacitor bank. The equations for s_{cr} and t_{cr} (as a function of B_C) have been verified using a dynamic-simulation model of the sample system. A severe three phase-to-ground fault has been created on the system such that the terminal voltage at the constant speed WTG should remain as per LVRT requirements. To consider the worst condition, the wind velocity has been kept constant at its rated value in the simulation. Therefore, the mechanical torque of the turbine will remain

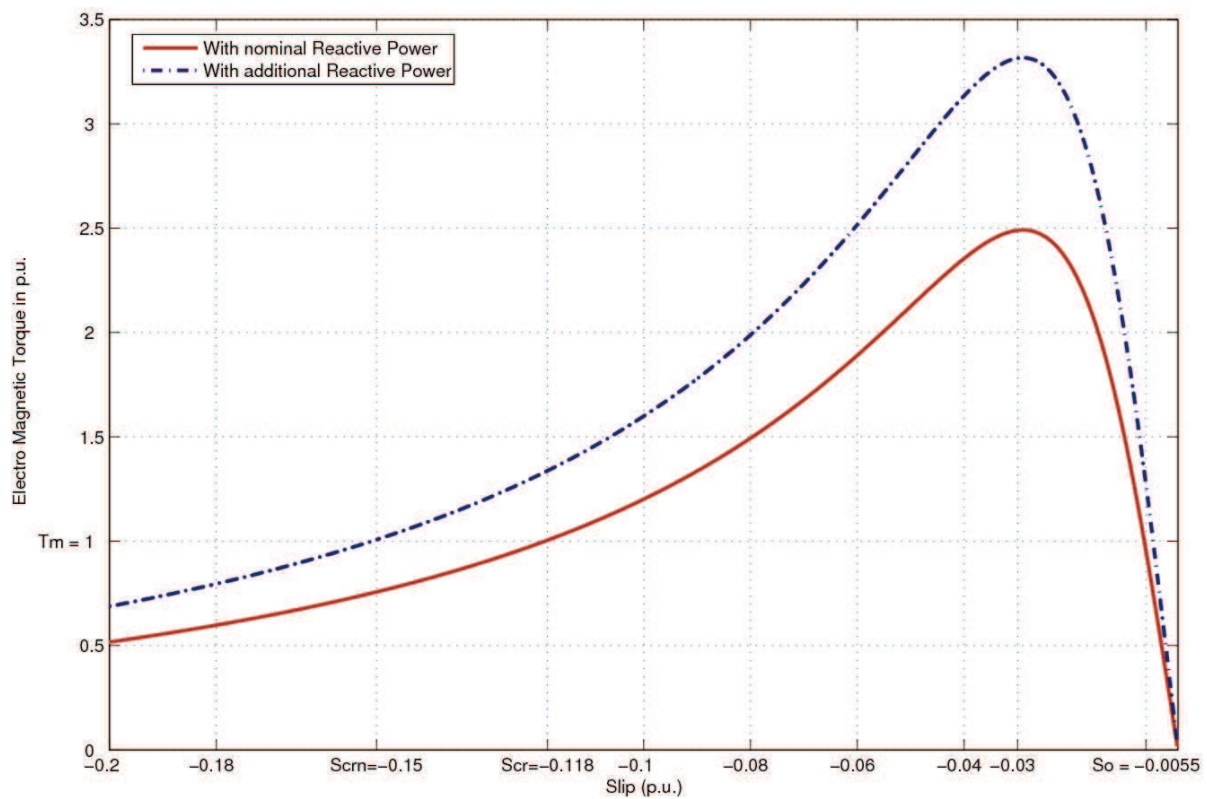


Fig. 6. Torque-slip characteristics of the WTG with nominal and additional reactive power.

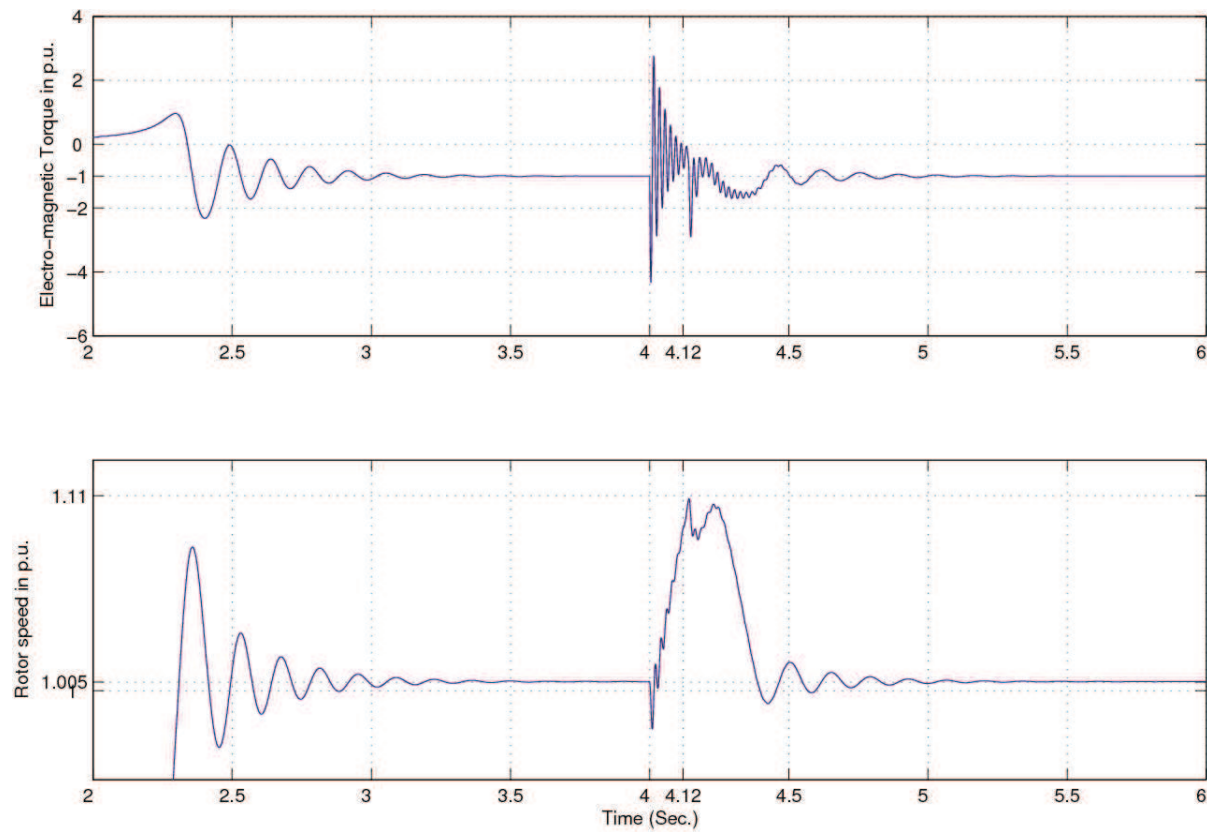


Fig. 7. Electromagnetic torque and rotor speed without additional capacitor bank.

at 1 p.u. during the fault. As per LVRT requirements (refer Fig. 1), a WTG should remain stable for 0.15 s with a terminal voltage of 0.15 p.u. It means that to satisfy the LVRT requirement, a WTG should have a critical clearing time of at least 0.15 s.

Fig. 7 shows the electromagnetic torque and rotor speed in per unit. During the fault, the value of T_e will reduce to almost zero. Hence, the rotor will accelerate to -0.11 p.u. slip within 0.12 s. The numerical values of the critical slip and time are calculated to be -0.118 p.u. and 0.12 s from equations (7) and (11) respectively. If the fault persist for more than the critical clearing time (0.12 s), the rotor will continue to accelerate and the WTG becomes unstable. Fig. 8 shows the electromagnetic torque and rotor speed for a fault of duration 0.15 s.

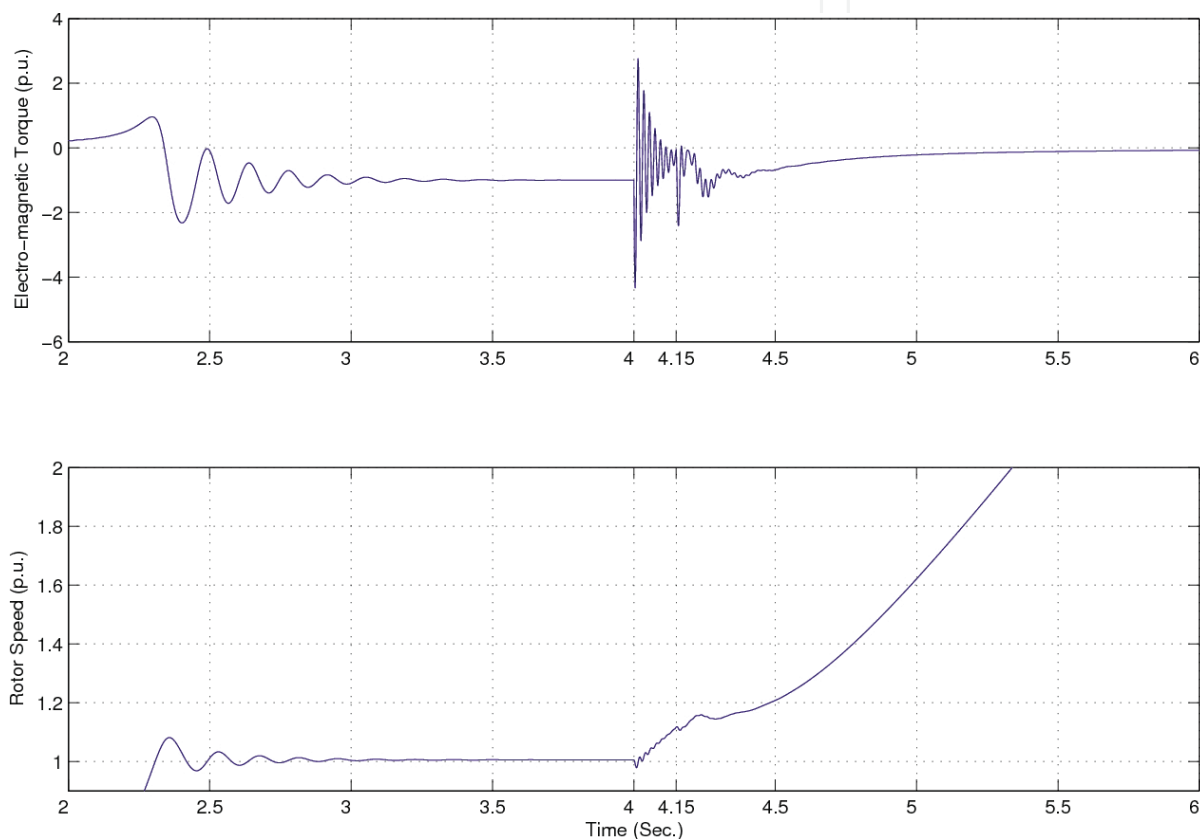


Fig. 8. Electromagnetic torque and rotor speed without additional capacitor bank for a fault of duration 0.15 s.

The speed of the WTG ramps up gradually and it has to be disconnected from the grid before the mechanical constraint on the rotor speed (1.2 p.u.) is reached. However, as per LVRT requirements, a constant speed WTG should remain connected for at least 0.15 s, which is not satisfied for this 600 kW WTG with a nominal value of reactive power compensation. To meet the LVRT requirements, an additional capacitor bank has been employed in parallel with the WTG. With this, executing the dynamic model again, it has been observed that the WTG remains stable even for 0.15 s. The rotor accelerates to -0.15 p.u. slip, and after the fault is cleared, the rotor comes back to its nominal value of -0.005 p.u. slip as shown in Fig. 9.

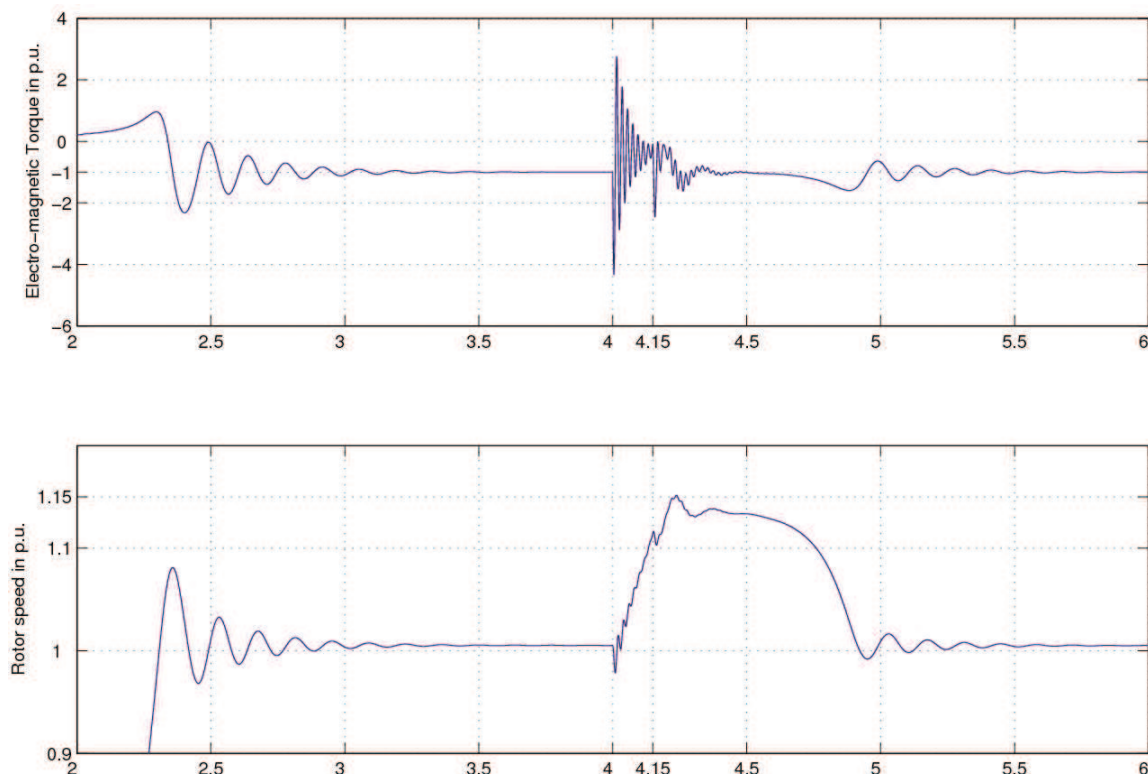


Fig. 9. Electromagnetic torque and rotor speed with additional capacitor bank.

3. Enhancement of rotor speed stability margin using active stall control

3.1 About active stall control

The rotor speed stability of a constant speed WTG can be improved by active stall control. Under transient conditions, the active stall controller controls the blade pitch angle (β) in the negative direction to reduce the turbine torque. This action helps to reduce the acceleration of the rotor, and improves the rotor speed stability. Using this phenomenon, the enhancement of rotor speed stability of a constant speed WTG with active stall is explained as follows. The active stall control based constant speed WTG has control of pitch in the negative direction (i.e. between -90° to 0°) with respect to pitch control based WTG (Type-A1). The rate of negative pitch control is normally less than 8° per second.

Fig. 10 shows the difference in the direction of blade rotation between pitch controlled and active stall controlled constant speed WTG. In the figure, the chord line is the straight line connecting the leading and trailing edges of an airfoil. The plane of rotation is the plane in which the blade tips lie as they rotate. The pitch angle (β) is the angle between the chord line of the blade and the plane of rotation. And, the angle of attack (α), is the angle between the chord line of the blade and the relative wind or the effective direction of air flow.

In active stall control, at low wind speeds, the machine is usually controlled by pitching its blades similar to a pitch controlled machine, to track maximum power generation. When the machine reaches its rated power value, the blades are pitched in the direction opposite from what a pitch controlled machine does, in order to reduce output power. This needs pitch angle β to be decreased, typically, by a small amount only. Hence, the rating of pitch drives is less for active stall control as compare with pitch control (Ackermann, 2005). Therefore, the cost and complexity are comparatively less for active stall controlled WTGs.

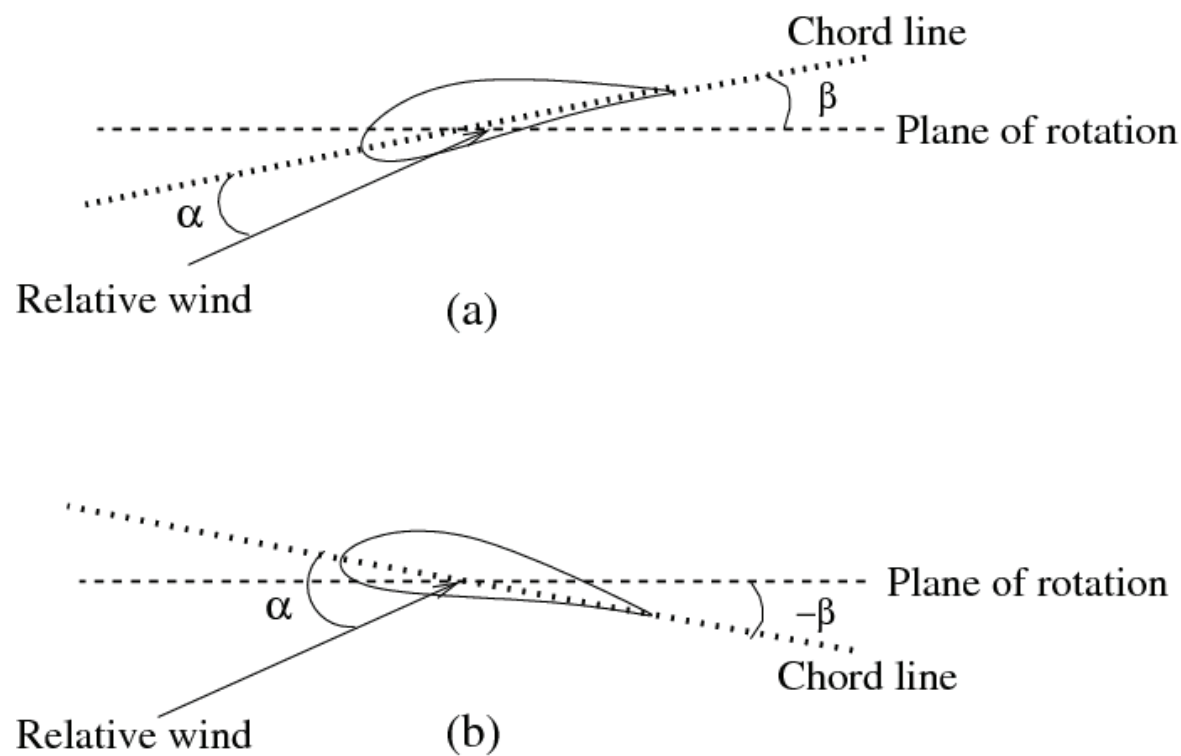


Fig. 10. Power generation control methods: (a) pitch control, (b) active stall control.

3.2 Design of active stall controller for constant speed WTG

The block diagram of active stall based WTG is shown in Fig. 11. To enhance rotor speed stability, pitch angle controller controls the generator speed by means of pitch angle of the blades. Accordingly, the mechanical torque (input to the induction generator) changes and it controls the rotor speed to lie within the allowable range.

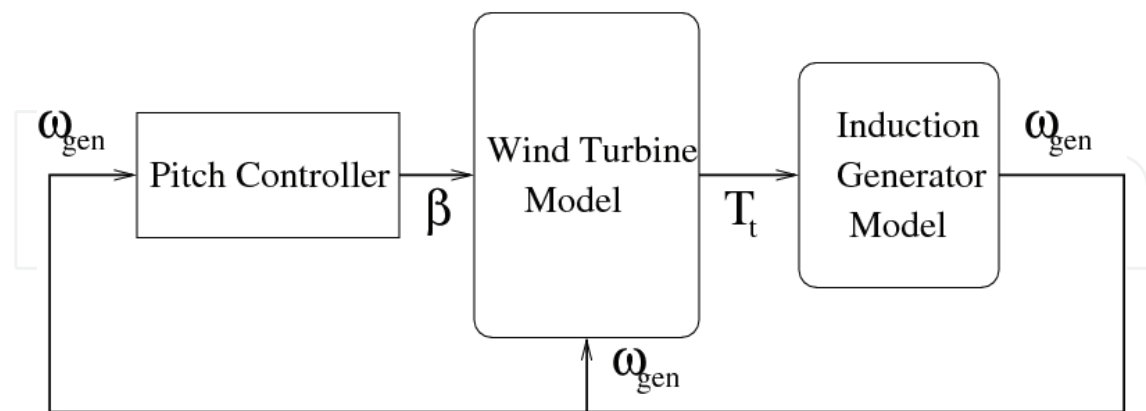


Fig. 11. Block diagram of active stall control based WTG.

As shown in Fig. 12, the pitch angle controller controls the pitch angle of the wind turbine blades. This would change the power coefficient C_p , which changes the mechanical torque input to the induction generator. Finally, the pitch angle controller controls the speed of the generator and enhances rotor speed stability. In the figure, T represents the time constant of the servo mechanism. The values of the controller parameters are given in Table 3.

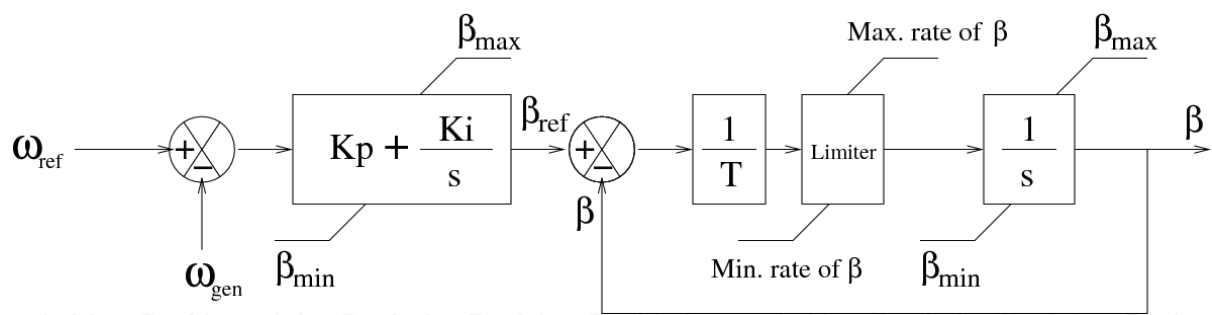


Fig. 12. Active stall pitch controller.

3.2.1 Aerodynamic model of the wind turbine

The aerodynamic torque developed on the main shaft of a wind turbine is give by:

$$T_a = \frac{1}{2\omega_m} \rho \pi R^2 V_w^3 C_p(\beta, \lambda) \tag{12}$$

where, T_a is the aerodynamic torque developed in $N \cdot m$; ω_m is the speed of the wind turbine in rad/s ; ρ is air density in kg/m^2 ; R is the radius of wind turbine blade rotation area in m ; V_w is the average wind speed in m/s ; C_p is the power coefficient of the wind turbine.

3.3 Simulation results and discussions

As shown in Fig. 13, a 1.5 MW constant speed WTG has been connected to a medium voltage (MV) distribution network. Modeling of WTG with capacitor bank connected to a sample system has been simulated using DlgSILENT PowerFactory.

Parameters	Value
Rated Power	1.5 MW
Rated Phase Voltage	690 V
Rated Frequency	50 Hz
Number of Poles	4
Stator Resistance (rs)	0.01 p.u.
Stator Leakage Reactance (Xls)	0.1 p.u.
Rotor Resistance (rr)	0.01 p.u.
Rotor Leakage Reactance (Xlr)	0.1 p.u.
Magnetizing Reactance (Xm)	3.0 p.u.
Inertia constant (J)	20.0 kg m ²

Table 2. Parameters of a 1.5 MW constant speed WTG

For rotor speed stability analysis, a 3-phase severe fault has been created on line-1 at time $t=5$ s. The fault has been cleared by removing that line from the system at time $t=5.15$ s. To analyze the behavior of the WTG during this grid disturbance, the quantities of induction generator (at bus-6) such as active power generation (in MW), rotor speed (in p.u.), reactive power generation (in Mvar), and generator terminal voltage (in p.u.) have been plotted. The effect of the operating point and active stall control on rotor speed stability is illustrated in

the next sub-sections. If a fault occurs close to a constant speed WTG, the voltage at the generator terminals of the wind turbine drops, which results in the reduction of active power. If a wind turbine controller does not attempt to reduce the mechanical power input, the turbine accelerates during the fault. If a wind turbine has no means of controlling its power, then critical clearing time will be very short (Ledesma et al., 2003). Figs. 14 and 15 show the induction generator quantities when a 3-phase line fault is created on Line-1 at 5 s and cleared at 5.15 s by disconnecting the line. During the fault, the voltage dips and active power generator reduce to almost zero. As the torque of wind turbine is not controlled, the generator rotor continue to accelerate. This result into the rotor speed instability. Finally, the over-speed relay removes the generator from the grid. Because of this phenomenon, it can be said that a constant speed (squirrel cage) induction generator does not have LVRT capability.

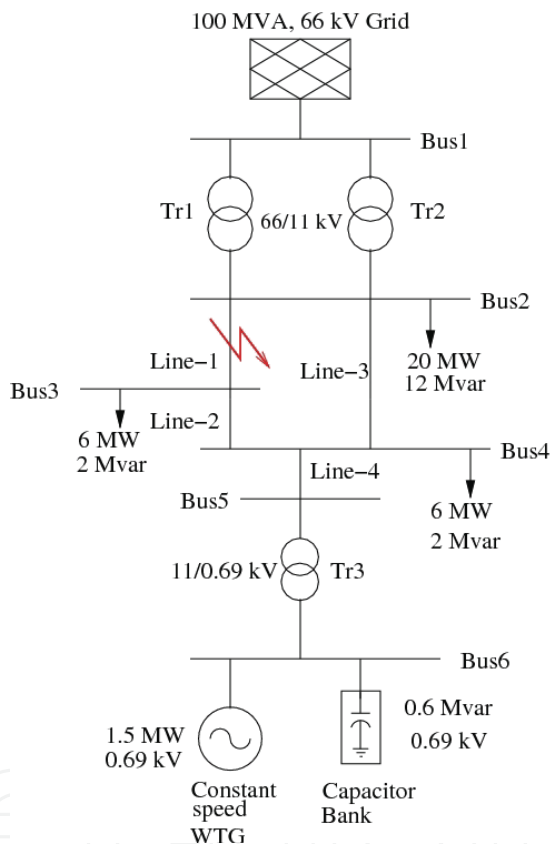


Fig. 13. A sample system with a 1.5 MW constant speed WTG.

Parameters	Value
Proportional gain (Kp)	500
Integral gain Ki	20
Time constant (T)	0.5s
Min. limit of β (β_{min})	-30°
Max. limit of β (β_{max})	10°
Rate of β	$8^{\circ}/s$

Table 3. Parameters of active stall controller

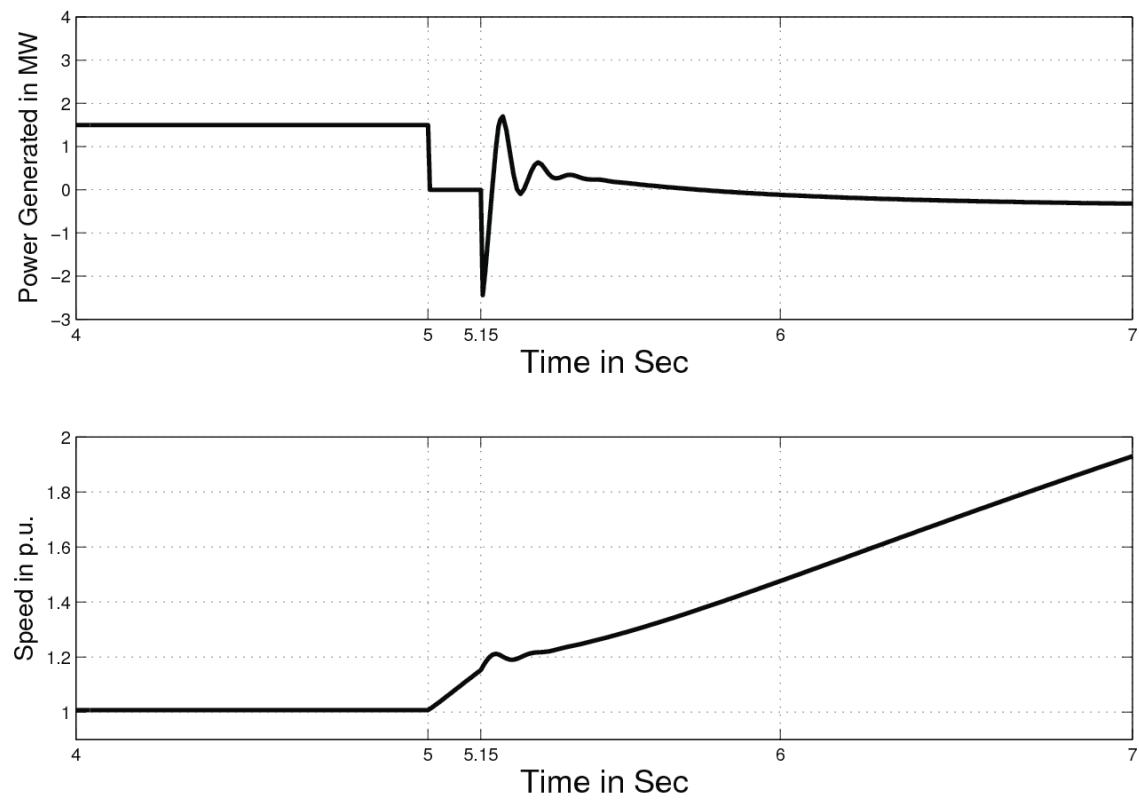


Fig. 14. Generator active power and speed without active stall control.

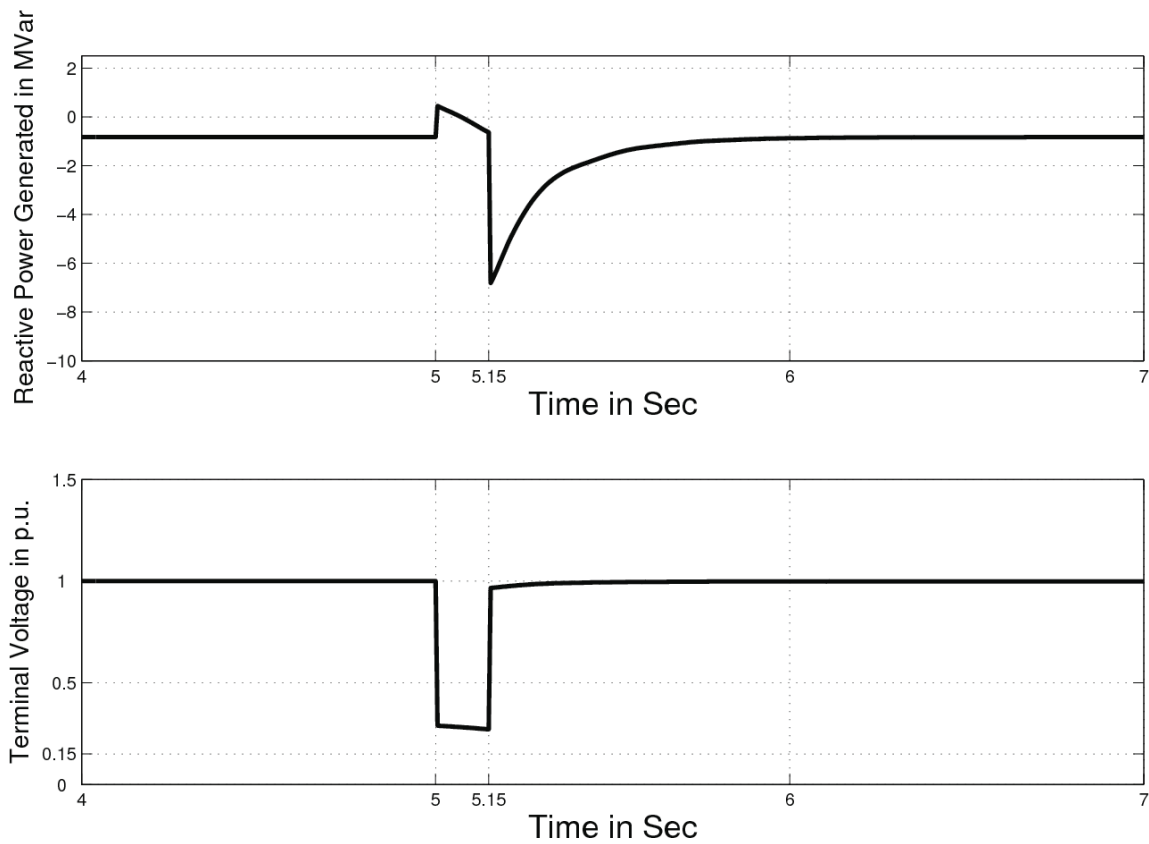


Fig. 15. Generator reactive power and terminal voltage without active stall control.

Parameters	Value
WTG mechanical inertial (J)	4x10 ⁶ kgm ²
Stiff coefficient(k)	100x10 ⁶ Nm/rad
Damping coe cient(D)	0 Nms/rad
Radius of blade rotation area (R)	35 m
Air density (ρ)	1.225kg/m ³

Table 4. Parameters of Wind Turbine

3.4 Effect of active stall control on the rotor speed stability

With the help of active stall control, the input mechanical torque of a constant speed WTG can be reduced. During a grid disturbance, the system voltage sags, and hence, the active power supplied by the WTG decreases. As a result, the rotor speed increases and the WTG draws a very high reactive power, as shown in Figs. 16 and 17. In this case, the WTG power output is 1.5 MW (at constant wind speed). Using active stall pitch controller, the WTG will remain stable even though the fault is cleared at 5.4 s. That is because the mechanical input power, and hence, the active power generated is reduced by controlling the pitch angle in negative direction. This results into reduction in mechanical input torque. Consequently, the speed and hence, the reactive power drawn reduces and this improves the rotor speed stability, as shown in Figs. 16 and 17. A constant speed WTG continues to supply power to the grid and satisfy the LVRT requirements of the WTG.

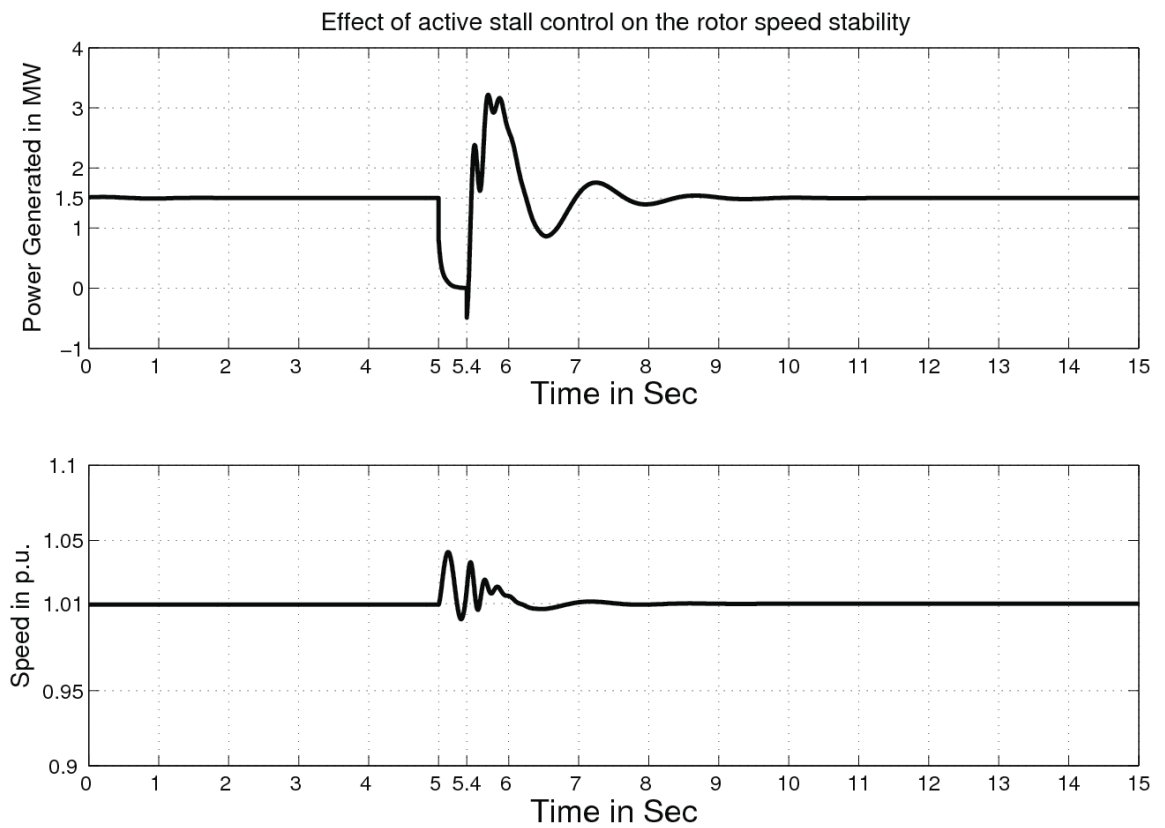


Fig. 16. Effect of active stall control on rotor speed stability: active power and speed.

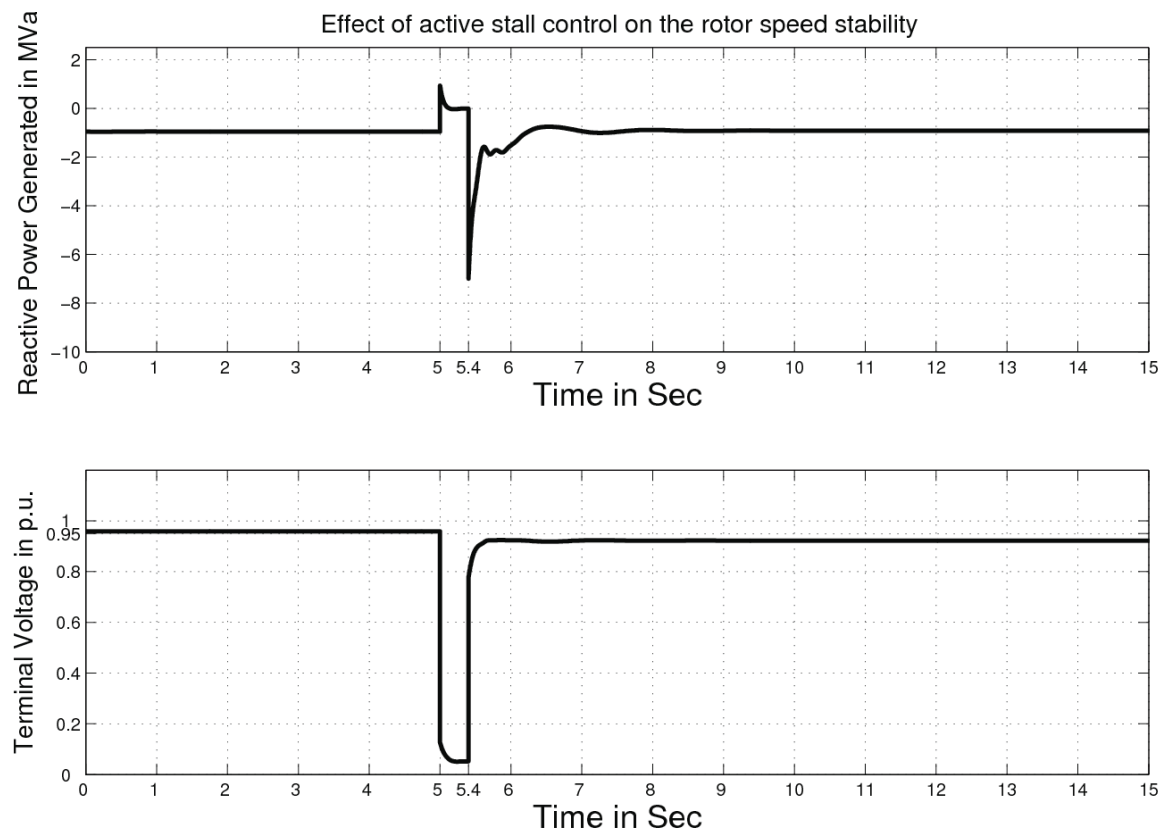


Fig. 17. Effect of active stall control on rotor speed stability: reactive power and voltage.

4. Conclusion

It has been shown that a constant speed WTG cannot meet LVRT grid code due to rotor speed instability. Consequently, the analysis has been aimed towards developing techniques to enhance the rotor speed stability such a way that a constant speed WTG can satisfy LVRT grid code.

The first technique involves providing additional reactive power support during disturbances. This technique is useful for a constant speed WTG without active stall control. This extra reactive power would recover the voltage and hence, the electromagnetic torque. Therefore, the rotor acceleration reduces and the value of t_{cr} increases. For this analysis, a 600 kW constant speed WTG connected to a sample network with nominal reactive power support ($B_C = 0.22$ p.u.) has been simulated using MATLAB. Using the simulation results, it has been shown that with this nominal value of reactive power support, t_{cr} is 0.12 s. However, according to the LVRT requirements t_{cr} should be at least 0.15 s. Therefore, additional reactive power support of the same value ($B_C = 0.22$ p.u.) has been connected. This extra reactive power increases the value of t_{cr} to 0.15 s, which is in compliance with the LVRT requirements.

Second technique is based on pitch angle control of turbine blades to control the mechanical torque. For this analysis, an active stall controller for use with turbine dynamic model has been designed using DIgSILENT simulation tool. From this simulation model, it has been shown that during a network disturbance, the active stall controller reduces the turbine torque and the rotor acceleration. Consequently, this would enhance the rotor speed stability margin. For this analysis, a 1.5 MW constant speed WTG connected to a sample

system has been simulated using DlgSILENT. From the simulation results, it has been shown that with the help of active stall control, the value of t_{cr} increases from 0.1 s to 0.4 s in order to meet LVRT requirements.

During grid integration, it is mandatory for the owners of WTGs to ensure compliance with the grid codes. This thesis work, therefore, can be useful for a utility or a regulatory commission to determine whether a particular constant speed WTG can meet the grid codes. Further, this work also presents techniques to enhance the rotor speed stability margin. These techniques can be helpful to manufacturers of constant speed WTGs to achieve compliance with grid codes such as LVRT requirements.

In this chapter, the study of rotor speed stability has been carried out for a constant speed WTG. This work can be extended by considering analysis for an aggregate model of wind farm with a number of such constant speed WTGs. In practice, wind farms can also be equipped with FACTS devices, such as, SVC and STATCOM in addition to capacitor banks on each WTG. The sizing of such FACTS devices can be determined to satisfy LVRT requirements for the aggregated wind farm by modifying the analysis for the enhancement of rotor speed stability.

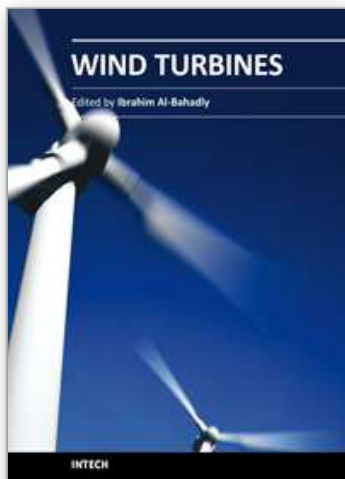
5. References

- Agalgaonkar, A.; Dobariya, C.; Kanabar, M. & Khaparde, S. A. (2006). Optimal sizing of Distributed Generation in MicroGrid, *Proceedings of IEEE international Power India Conference*, ISBN: 10.1109/POWERI.2006.1632627, April 2006, IEEE, New Delhi.
- Zavadil, R.; Miller, N.; Ellis, A. & Muljadi, E. (2005). Making connections, *IEEE Power Energy Magazine*, pp. 26–37, Nov. 2005.
- Ackermann, T. (2005). *Wind Power in Power Systems*. John Wiley & Sons Ltd., ISBN 0470855088, England.
- Kanabar, M. & Khaparde, S. A. (2008). Evaluation of Rotor Speed Stability Margin of a Constant Speed Wind Turbine Generator, *Proceedings of IEEE international Power India Conference*, ISBN: 10.1109/ICPST.2008.4745277, Oct. 2006, IEEE, New Delhi.
- Wind Power India Website (2010). [Online]. Available: <http://www.windpowerindia.com>.
- Kanabar, M.; Dobariya, C. & Khaparde, S. A. (2006). Rotor Speed Stability Analysis of Constant Speed Wind Turbine Generators, *Proceedings of IEEE conference on Power Electronics Drives and Energy Systems*, ISBN: 10.1109/PEDES.2006.344270, Dec. 2006, IEEE, Delhi.
- Samuelsson, O. & Lindahl, S. (2005). On speed stability, *IEEE Transaction on Power System*, Vol. 20, No. 2, May 2005, pp. 1179–1180, ISSN : 10.1109/TPWRS.2005.846194.
- Rodriguez, J. M.; Fernandez, J. L.; Beato, D.; Iturbe, R.; Usaola, J.; Ledesma, P. & Wilhelmi, J. R. (2002). Incidence on power system dynamics of high penetration of fixed speed and doubly fed wind energy systems: study of the Spanish case, *IEEE Transaction on Power System*, Vol. 17, No. 4, Nov. 2002, pp. 1089–1095, ISSN : 10.1109/TPWRS.2002.804971.
- Nunes, M. V. A.; Bezerra, U. H. & Zurn H. H. (2003). Transient stability margin of variable versus fixed speed wind systems in electrical grids, *Proceedings of IEEE Power Tech.*, ISBN: 10.1109/PTC.2003.1304460, June 2003, IEEE, Bologna.
- Chompoo-inwai, C.; Yingvivatanapong, C.; Methaprayoon, K. & Lee, W. J. (2005). Reactive compensation techniques to improve the ride-through capability of wind turbine

- during disturbance, *IEEE Transaction on Industry Applications*, Vol. 41, No. 3, May 2005, pp. 666–672, ISSN : 10.1109/TIA.2005.847283.
- Jenkins, N.; Allan, R.; Crossley, P.; Kirschen, D. & Strbac, G. (2000). *Embedded Generation*. The Institution of Electrical Engineers, ISBN: 0852967748, England.
- Ledesma, P.; Usaola, J. & Rodriguez, J. L. (2003). Transient stability of a fixed speed wind farm, *Renewable Energy*, Vol. 28, pp. 1341–1355, May 2003.

IntechOpen

IntechOpen



Wind Turbines

Edited by Dr. Ibrahim Al-Bahadly

ISBN 978-953-307-221-0

Hard cover, 652 pages

Publisher InTech

Published online 04, April, 2011

Published in print edition April, 2011

The area of wind energy is a rapidly evolving field and an intensive research and development has taken place in the last few years. Therefore, this book aims to provide an up-to-date comprehensive overview of the current status in the field to the research community. The research works presented in this book are divided into three main groups. The first group deals with the different types and design of the wind mills aiming for efficient, reliable and cost effective solutions. The second group deals with works tackling the use of different types of generators for wind energy. The third group is focusing on improvement in the area of control. Each chapter of the book offers detailed information on the related area of its research with the main objectives of the works carried out as well as providing a comprehensive list of references which should provide a rich platform of research to the field.

How to reference

In order to correctly reference this scholarly work, feel free to copy and paste the following:

Mitalkumar Kanabar and Srikrishna Khaparde (2011). Rotor Speed Stability Analysis of a Constant Speed Wind Turbine Generator, Wind Turbines, Dr. Ibrahim Al-Bahadly (Ed.), ISBN: 978-953-307-221-0, InTech, Available from: <http://www.intechopen.com/books/wind-turbines/rotor-speed-stability-analysis-of-a-constant-speed-wind-turbine-generator>

INTECH
open science | open minds

InTech Europe

University Campus STeP Ri
Slavka Krautzeka 83/A
51000 Rijeka, Croatia
Phone: +385 (51) 770 447
Fax: +385 (51) 686 166
www.intechopen.com

InTech China

Unit 405, Office Block, Hotel Equatorial Shanghai
No.65, Yan An Road (West), Shanghai, 200040, China
中国上海市延安西路65号上海国际贵都大饭店办公楼405单元
Phone: +86-21-62489820
Fax: +86-21-62489821

© 2011 The Author(s). Licensee IntechOpen. This chapter is distributed under the terms of the [Creative Commons Attribution-NonCommercial-ShareAlike-3.0 License](https://creativecommons.org/licenses/by-nc-sa/3.0/), which permits use, distribution and reproduction for non-commercial purposes, provided the original is properly cited and derivative works building on this content are distributed under the same license.

IntechOpen

IntechOpen